Impacts of Cooperative Adaptive Cruise Control on Freeway Traffic Flow

Steven E. Shladover, Dongyan Su, and Xiao-Yun Lu

This study used microscopic simulation to estimate the effect on highway capacity of varying market penetrations of vehicles with adaptive cruise control (ACC) and cooperative adaptive cruise control (CACC). Because the simulation used the distribution of time gap settings that drivers from the general public used in a real field experiment, this study was the first on the effects of ACC and CACC on traffic to be based on real data on driver usage of these types of controls. The results showed that the use of ACC was unlikely to change lane capacity significantly. However, CACC was able to increase capacity greatly after its market penetration reached moderate to high percentages. The capacity increase could be accelerated by equipping non-ACC vehicles with vehicle awareness devices so that they could serve as the lead vehicles for CACC vehicles.

An earlier phase of this project included a field test of adaptive cruise control (ACC) and cooperative adaptive cruise control (CACC) systems driven by 16 drivers from the general public. Those drivers were encouraged to select the time gap settings that they preferred for each system, and their selections of time gap were recorded, along with many other parameters, for subsequent analysis. They were also surveyed to determine their subjective opinions about the ACC and CACC systems. The results of this experiment were encouraging about the potential market acceptance of ACC and CACC when they are made available to the general public. These results were reported in two prior project reports (*1, 2*) and two technical papers (*3, 4*).

The ACC–CACC field test produced quantitative results indicating the relative preferences of the driving population for operating at the different available time gap settings. These time gap preferences can have a significant influence on traffic flow and highway lane capacity. The work reported here uses a traffic microsimulation based on the ACC–CACC field test results to produce the first authoritative quantitative estimates of the impacts that these systems could have on highway capacity.

The maximum traffic flow is determined by admissible time gaps between vehicles. The admissible time gap is determined by the means of controlling the vehicle's car-following behavior: manual driving, ACC, or CACC. In manual driving, the acceptable time gap is determined on the basis of the driver's perception of what is safe, including his or her perception and reaction time, and is influenced by the driver's experiences, including expectations about the behavior of other drivers, especially the driver of the leading vehicle. Vehicles with ACC or CACC have discrete time gap settings, which the driver can select based on his or her perceptions of the capabilities of the system. The net effect on traffic depends on whether drivers have sufficient confidence in the ACC–CACC systems to select time gaps that differ significantly from the gaps they use in manual driving.

This research evaluates the effects of the use of ACC and CACC on freeway capacity by microscopic simulation based on the actual gaps that the drivers selected in the field testing of these systems. The simulation platform for this study is the commercially available traffic microsimulation program AIMSUN, which was selected because it was the only simulation platform in which the NGSIM model of oversaturated freeway flow could be implemented to provide the most realistic representation of normal drivers' car-following behavior in dense traffic.

The field test of CACC (*1–4*) was motivated by a simulation study that was conducted 10 years ago and showed that if drivers were comfortable using CACC at a time gap of 0.5 s, the capacity per lane could be increased to as high as 4,400 vehicles per hour (vph) if all vehicles were equipped with the system (*5, 6*). However, the field study was needed to determine which gaps the drivers would find acceptable. At the time of the original simulation study (*5, 6*), several papers had already been published in which a variety of modeling approaches were used to estimate the highway capacity implications of ACC, producing widely varying estimates of capacity because of significantly different assumptions about the car-following behavior of drivers and ACC systems. Those earlier studies were reviewed in the published papers (*5, 6*).

During the past 10 years there have been a few additional studies estimating the impacts that ACC and CACC could have on traffic flow, but none have yet had the benefit of real experimental data about how drivers actually use these systems on the highway. Van Arem et al. used the MIXIC microscopic simulation to investigate the traffic throughput and stability impacts of CACC, incorporating good vehicle dynamics and driver behavior models (*7*). They studied a freeway lane drop as the disturbance to induce a shock wave to limit capacity and found that the shock wave effect could be mitigated and the average speed increased with higher market penetrations of CACC. Their predictions of CACC impacts are generally consistent with the results that are shown here, with significant capacity increases at the higher market penetration levels.

Kesting et al. simulated ACC with infrastructure-determined set speeds, a form of infrastructure-cooperative ACC rather than vehicle-cooperative ACC (*8, 9*). Their intelligent driver model (IDM) showed that a 25% market penetration of these ACC vehicles could eliminate congestion (and even 5% could produce noticeable improvements in travel times) for the specific peak-period traffic scenario that they chose to simulate, but this congestion benefit appears to be attributable to the variable speed limit strategy that

California Partners for Advanced Transportation Technology, University of California, Berkeley, Richmond Field Station, Building 452, 1357 South 46th Street, Richmond, CA 94804-4648. Corresponding author: S. E. Shladover, steve@path.berkeley.edu.

Transportation Research Record: Journal of the Transportation Research Board, No. 2324, Transportation Research Board of the National Academies, Washington, D.C., 2012, pp. 63–70.
DOI: 10.3141/2324-08

they adopted rather than to the car-following dynamics of the ACC system. They did not directly consider the impacts that ACC would have on the achievable capacity. Schakel et al. used a modified version of IDM (which they called IDM+) to explore the implications on traffic flow stability of CACC and an acceleration advice controller, which advises the driver when to accelerate and decelerate rather than doing so automatically (*10*). They included results of a field experiment using 50 vehicles equipped with that controller, showing reductions in variability of speeds and gaps between vehicles. Their CACC design was focused on improving traffic flow stability rather than on increasing capacity, so they did not directly address the capacity issue.

Kesting et al. hypothesized an idealized car-following model designed to dampen traffic disturbances and then assumed that this model would represent ACC driving, even though it does not correspond to real ACC system behavior (*11*). They simulated combinations of vehicles represented by this model with other vehicles driven by their IDM car-following model (which incorporates unrealistically hard braking in response to vehicles that cut in) and assumed that the model would represent conventionally driven vehicles. As they increased the market penetration of the idealized ACC vehicles in their simulations, they showed significant increases in bottleneck traffic flow compared with the case in which all vehicles were driven by the IDM model, but both of their car-following models were sufficiently unrealistic that this study sheds little light on the flow rates that could be achieved with or without ACC.

VEHICLE TYPES TO BE SIMULATED

Four vehicle types are represented in the simulation to accommodate all possible combinations of vehicles that could be interacting with each other in ways that would influence freeway traffic flow and capacity:

1. Manual vehicle. Vehicle is driven manually with car-following behavior represented by the NGSIM oversaturated flow model.
2. ACC vehicle. Vehicle has control in which car following is determined on the basis of a simple first-order control law representing the behavior of a typical ACC system, with relatively slow, gentle responses to changes by the car ahead.
3. Here I am! (HIA) vehicle. Vehicle is driven manually just like the manual vehicle but equipped with a dedicated short-range communications radio that frequently broadcasts a "here I am" message giving its location and speed. If it is being followed by a CACC vehicle, that following vehicle can use its CACC.
4. CACC vehicle. If this vehicle is following an HIA vehicle or another CACC vehicle, it can use its CACC car-following capability. If it is following a manual vehicle or an ACC vehicle, it acts like another ACC vehicle. The CACC car-following capability includes a faster response to changes by the car ahead and permits following at significantly shorter time gaps, based on the gap values chosen by drivers in the field test (*2–4*).

Differences in the behavior of car-following models account in large part for the wide range of effects that have been predicted in previous studies of the effects of ACC on traffic flow. The models of conventional car following are still not fully mature, but a state-of-the-art model was chosen that has been calibrated on the basis of real microscopic freeway traffic data, as explained later in the section on the manual driving model.

ACC systems developed by different manufacturers display a considerable variety of performance characteristics based on the limitations of their sensors and on the different performance objectives their designers have adopted in trying to match them to the personalities and market segments of their host vehicles. The detailed car-following logic of these systems is proprietary to their developers, representing valuable intellectual property, so this logic is not publicly available. Some of them drive like aggressive drivers and some like timid drivers; there is no uniform standard for their dynamic response. Indeed, recent tests of ACC systems from five Japanese automobile companies (unfortunately not yet documented in the technical literature but presented informally in a panel session at the 18th World Congress on Intelligent Transportation Systems, held in Orlando, Florida, in October 2011) have shown this diversity of dynamic responses quantitatively and have indicated potential challenges when vehicles with incompatible car-following behavior are driven one behind the other.

Considering this diversity of ACC behavior and the shortage of public documentation of the car-following dynamics of real ACC vehicles, a simple first-order dynamic response for ACC car following was adopted. From a vehicle dynamics perspective, this choice could be considered somewhat optimistic because it is more stable than the actual responses of ACC systems, which have substantial transport lags (in the range of a half to a full second) associated with the limitations of their sensor signal-processing systems. This analysis concentrates on steady-state car-following behavior rather than on the dynamics associated with large speed changes in bottleneck conditions because in those more severe conditions it is generally necessary for the driver to intervene and take over control from the ACC, which makes the combined ACC and driver manual dynamics extremely complicated and diverse. The prior simulation studies that have attempted to represent ACC performance in bottlenecks have ignored this problem and have instead assumed ACC systems to be braking harder than any real ACC systems can brake [twice as hard as the maximum ACC braking permitted by ISO 15622 in the case of the study by Kesting et al. (*11*)].

MICROSIMULATION PLATFORM

The simulation was built on AIMSUN, which contains microscopic and mesoscopic simulators, a dynamic traffic simulator, and macroscopic and static assignment models (*12*). It also offers extended tools for advanced investigation, like the AIMSUN software development kit, AIMSUN application programming interface, and AIMSUN MicroSDK. The AIMSUN microscopic simulator, application programming interface, and MicroSDK were used in this project.

The AIMSUN microscopic simulator is the tool used to construct traffic networks, define vehicle types and their basic properties, specify traffic demand and traffic control, and run the simulations (*13*). For this project, the geometry of the freeway and its speed limit and the four vehicle types and their properties, such as length and width, are defined in the AIMSUN microscopic simulator.

The AIMSUN application programming interface module is an interface that allows external applications to exchange data with AIMSUN during simulation (*14*). The user can obtain necessary information during simulation, such as the measurements of a detector or the state of a particular vehicle. The user can also control the traffic, determining when and how a new vehicle enters the network.

The microscopic software development kit is the tool used to implement new behavioral models in the AIMSUN simulation, replacing the default driver model in AIMSUN (*15*). The new driver behavior is implemented by the plug-in, which is a DLL file generated after some C++ files are built. During each simulation step, AIMSUN calls the functions in the plug-in and updates the driver behavior on the basis of the user-defined model. The new driver behavior models that were developed here to represent manually driven, ACC, and CACC vehicles were programmed in MicroSDK.

CONTROL ALGORITHMS FOR ACC AND CACC VEHICLES

The following variables are used to define the vehicle-following control algorithms for ACC or CACC vehicles discussed in this section. These are simplified representations of the ACC and CACC car-following rules that were actually implemented on the test vehicles for the field experiments. The ACC car-following rules are proprietary to Nissan, and the CACC car-following behavior was described by Bu et al. (*16*). Simpler representations were needed here for computational efficiency because they need to be executed many times in each simulation and also because the finer details of the actual car-following dynamics of these systems were implemented for driver comfort but probably have little influence on traffic flow dynamics.

The variables used are as follows:

v = speed of controlled ACC–CACC vehicle (m/s),
v_d = desired speed set by driver or speed limit of road (m/s),
v_e = speed error (m/s),
a_{sc} = acceleration by speed control (m/s^2),
s = spacing between controlled vehicle and its leading vehicle (m),
s_d = desired spacing (m),
s_e = spacing error (m), and
T_d = desired time gap (s).

The ACC and CACC vehicles have similar control algorithms, with the difference being in their desired time gaps. There are two modes, speed control and gap control, in the ACC–CACC control algorithm. The goal of speed control is to keep the vehicle speed close to the speed limit and that of gap control is to maintain the desired gap between the controlled vehicle and its leading vehicle. Speed control is activated when the spacing to the preceding vehicle in the same lane is larger than 120 m, and gap control is activated when the spacing is smaller than 100 m. If the spacing is between 100 m and 120 m, the controlled vehicle retains the previous control strategy to provide hysteresis and avoid dithering between the two strategies. These fixed distances for transitions are appropriate for operations at or near full highway speed, but for lower-speed operations these distances should be smaller.

In speed control, the control law is

$$v_e = v - v_d \tag{1}$$

$$a_{sc} = \text{bound}\left(-0.4 \cdot v_e, 2, -2\right) \tag{2}$$

$$a = a_{sc} \tag{3}$$

where the function "bound ( )" is defined as bound (x, x_{ub}, x_{lb}) := max(min(x, x_{ub}), x_{lb}) and ub is upper bound and lb is lower bound. The values +2 and −2 in Equation 2 are the maximum acceleration and deceleration of the vehicle under ACC–CACC control in units of meters per second squared. This control law tries to eliminate the error between the vehicle speed and the ACC set speed if the vehicle is in the speed control mode, with a time constant of 2.5 s, representing a typical gentle ACC response.

In gap control, the control law is based on maintaining a constant time gap between vehicles, which is typical of ACC vehicle-following strategies and well accepted by drivers because of its general similarity to drivers' own vehicle-following behavior:

$$v_e = v - v_d \tag{4}$$

$$a_{sc} = \text{bound}\left(-0.4 \cdot v_e, 2, -2\right) \tag{5}$$

$$s_d = T_d \cdot v \tag{6}$$

$$s_e = s - s_d \tag{7}$$

$$a = \text{bound}\left(\dot{s} + 0.25 \cdot s_e, a_{sc}, -2\right) \tag{8}$$

The +2 and −2 in Equations 5 and 8 have the same meaning as in speed control. This control law forces the vehicle to approach its desired time gap set point in gap control. But the vehicle will still obey the speed limit in gap control because if the commanded vehicle speed is larger than the set speed, this control law abides by the set speed, even if the current gap is larger than its desired gap.

MANUAL DRIVING MODEL

The manual driver behavior model is the NGSIM oversaturated freeway flow model developed by Yeo (*17*) and Yeo et al. (*18*). The NGSIM oversaturated freeway flow model contains car-following and lane-changing models, but only the car-following model was used, the CF mode in the work by Yeo (*17*) and Yeo et al. (*18*), because there is no lane changing in this simulation. The following variables are used in the manual driving model:

x_n^U, x_n^L = upper bound and lower bound for clearance between vehicles (m),
t = time,
n = vehicle sequence ID,
T^w = kinematic wave travel time (s),
g_n^{jam} = jam gap (m),
l = length of vehicle (m),
a = acceleration of vehicle (m/s^2),
v = speed of vehicle (m/s),
x = position of vehicle (m), and
v^f = free-flow speed (m/s).

The basic car-following model comes from Newell's linear model. It can be described as follows:

$$x_n\left(t + \Delta t\right) = \max\left\{x_n^U\left(t + \Delta t\right),\ x_n^L\left(t + \Delta t\right)\right\} \tag{9}$$

$$x_n^U\left(t + \Delta t\right) = \min\left\{\begin{array}{l} x_{n-1}\left(t + \Delta t - T_n^w\right) - l_{n-1} - g_n^{\text{jam}}, \\ x_n\left(t\right) + v_n\left(t\right)\Delta t + a_n^U \Delta t^2,\ x_n\left(t\right) + v_n^f \Delta t, \\ x_n\left(t\right) + \Delta x_n^s\left(t + \Delta t\right) \end{array}\right\} \tag{10}$$

$$x_n^L\left(t + \Delta t\right) = \max\left\{x_n\left(t\right) + v_n\left(t\right)\Delta t + a_n^L \Delta t^2,\ x_n\left(t\right)\right\} \tag{11}$$

$$\Delta x_n^s(t+\Delta t)=\Delta t\left(a_n^L T_n^w+\sqrt{\left(a_n^L T_n^w\right)^2-2a_n^L\begin{pmatrix}x_{n-1}(t)-x_n(t)\\-\left(l_{n-1}+g_n^{\text{jam}}\right)+d_{n-1}(t)\end{pmatrix}}\right) \tag{12}$$

$$d_{n-1}(t)=-\frac{v_{n-1}^2(t)}{2a_{n-1}^L} \tag{13}$$

The kinematic wave travel time in congested traffic conditions, T^w, is equivalent to the ACC time gap, with an offset to account for the minimum spacing at jam density.

This NGSIM oversaturated freeway flow model was calibrated by using the NGSIM data (*19*).

FREEWAY SECTION MODEL WITH SIMPLIFIED ROAD GEOMETRY

The simulated road is a one-lane straight freeway with speed limit of 105 km/h (65 mph). The freeway is 6.5 km long, and there is a detector 6 km from the entrance. This location is selected to make sure that all the flow measurements are in a steady state. The freeway is empty before the simulation. During the simulation, the entering of new vehicles is controlled by an algorithm written in the application programming interface file, which will be described subsequently. The total simulation length is 1 h, and the simulation step is 0.1 s. The flow is recorded at intervals of 5 min, but the first measurement is discarded because the first 5 min are viewed as the warm-up time. The capacity is the average flow during the remaining 55 min.

The four types of vehicles have the same physical characteristics, with a length of 4.7 m and width of 1.9 m. The accelerations are bounded within ±2 m/s^2.

In the simulation, the type of the next entering vehicle is randomly chosen but follows the percentages defined in the simulation cases to be tested. The desired time gap of the entering vehicle is also random. For manual driving, the randomness is introduced by the randomness of g_n^{jam}.

The maximum flow for manually driven vehicles on this type of simple freeway link should be about 2,200 vph, so the desired headway for manual driving is assumed to be 1.64 s (≈3,600/2,200 vph). The desired time gaps of the ACC or CACC vehicles were selected from the gaps actually selected by drivers in the field test (*1–4*):

- ACC: 31.1% at 2.2 s, 18.5% at 1.6 s, 50.4% at 1.1 s, and
- CACC: 12% at 1.1 s, 7% at 0.9 s, 24% at 0.7 s, and 57% at 0.6 s.

The difference between headway and time gap needs to be accounted for by incorporating the incremental time needed to travel the vehicle length at the defined operating speed.

The desired entering headways for the ACC and CACC vehicles are chosen on the basis of these time gaps, with the addition of the time increment to account for vehicle length. The gap for manual driving is selected randomly during the simulation, within a ±10% error range of 1.64 s, that is, from 1.48 to 1.8 s. At each simulation step, the travel time from the entrance to the location of the last entering vehicle is checked, based on the speed of that vehicle at that step. If this travel time is larger than the desired entering time gap, a new vehicle is allowed to enter the freeway at the same speed as its leading vehicle at that step. By this algorithm, the vehicles enter the freeway at an interval and speed that will not generate a measured maximum flow lower than the real capacity due to insufficient demand, and collisions associated with entering at too high a speed or too small a time gap are prevented.

Because the entering time gap for manually driven vehicles usually does not match their desired time gap, the manually driven vehicles need to adjust their speeds after they enter the freeway. This adjustment causes the vehicles following them, whether they are manual, ACC, or CACC, to also need to adjust speeds. By this process, small disturbances are introduced into the simulation. The simulated maximum flows should be achievable and stable in traffic with small disturbances.

SIMULATION SCENARIOS AND RESULTS

Simulation scenarios were defined to represent diverse combinations of manually driven, ACC, CACC, and HIA vehicles so that the effects of changes in market penetration of each kind of vehicle could be determined. For each scenario, three simulations were run with different random number seeds and the results of those simulations were averaged to produce the estimates of achievable traffic flow.

The all-manual case was already referenced as a base case with a nominal capacity that could potentially approach 2,200 vph per lane (vphpl). Allowing for the disturbances in vehicle motions and the diversity of driver gap selections, the simulations produced an average capacity of 2,018 vphpl with all-manual driving. When basic ACC vehicles were incorporated into the traffic stream, the achievable traffic flow appeared to be remarkably insensitive to the market penetration of ACC vehicles, with flow remaining within the narrow range from 2,030 to 2,100 vph regardless of the market penetration. This finding is a consequence of the similar driver preferences for ACC time gap settings to the time gaps that they adopt when they drive manually. This finding contradicts the results in some published papers (*8, 11*), which contend that ACC could substantially increase highway capacity.

If only the combinations of manually driven and CACC vehicles are considered, the trend in highway lane capacity with respect to CACC market penetration is as shown in the lower part of the histograms in Figure 1. This trend has a quadratic shape, based on

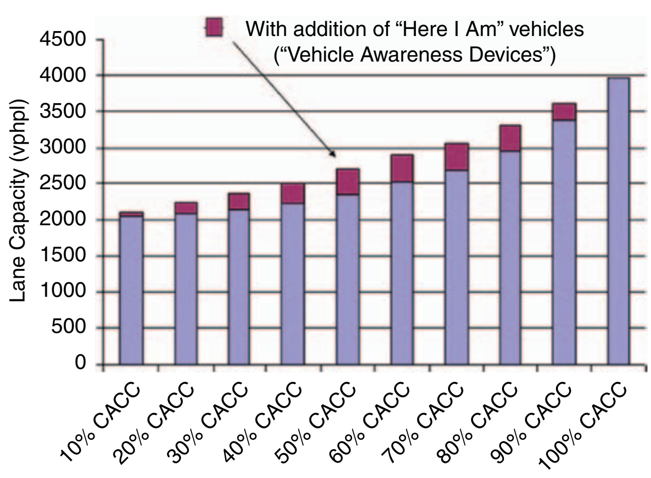

FIGURE 1 Highway lane capacity as function of changes in CACC market penetration relative to manually driven vehicles or vehicles with a vehicle awareness device.

the fact that the CACC vehicle can only use its CACC capability when it is following another CACC vehicle, but when it is following a manual vehicle it must revert to conventional ACC control. As a result, the capacity grows slowly until the CACC market penetration becomes substantial, and then it grows more rapidly. If all vehicles in a lane were equipped with CACC capability and the drivers chose the same distribution of CACC time gaps as they chose in the field test, the lane capacity would increase to 3,970 vph, a dramatic improvement.

One of the strategies being proposed in the U.S. Department of Transportation's Connected Vehicles Initiative to improve the performance of cooperative systems at low market penetrations is to equip as many existing vehicles as possible with a simple and inexpensive aftermarket positioning and communication onboard unit called a vehicle awareness device (VAD), which can broadcast an HIA message. This message provides the basic Global Positioning System coordinates and vehicle speed and heading information so that the onboard units on other vehicles can detect the trajectory of the vehicle. This information, if it is sufficiently accurate, would enable a VAD-equipped vehicle to be the leader for a CACC vehicle to follow at a short time gap. The effects of replacing the manually driven vehicles with VAD vehicles are shown in the upper segments of the histograms of Figure 1. In this case, all the vehicles that do not have CACC are equipped with the VAD and can therefore serve as leaders for the CACC vehicles. With this change, the quadratic growth becomes more nearly linear, and the capacity of the highway lane can be increased more significantly even at modest CACC market penetrations. At a 20% market penetration, the HIA addition increases capacity by 7%, at 30% market penetration it increases by more than 10%, and in the 50% to 60% market penetration range the increase is in the range of 15% compared with the cases without VADs.

In earlier studies of CACC before the current project, the effects of the different combinations of ACC and CACC market penetrations were simulated on the basis of the assumption that the CACC vehicles would be driven at 0.5-s time gaps (*5, 6*). This assumption produced a three-dimensional plot of achievable highway lane capacity that is reproduced here as Figure 2. The new simulation results, based on the time gaps that drivers actually chose in the field test, are shown in Figure 3 and Table 1. These capacity estimates are somewhat lower, with the 80% CACC–20% ACC result now in the range of 3,000 rather than 3,500 vph, for example.

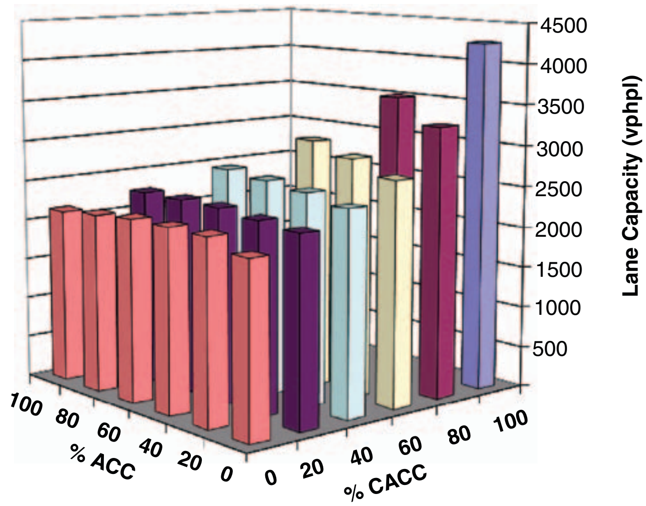

FIGURE 2 Original prediction of lane capacity effects of ACC and CACC vehicles driven at 0.5-s time gap from 2001 (*5, 6*).

The capacity effects of different combinations of CACC vehicles and VAD vehicles (with the rest being manually driven) are shown in Figure 4 and Table 2. As the market penetration of CACC increases, the increasing capacity attributable to the additional VAD vehicles can be seen, but it is a relatively subtle effect. For completeness, the analogous results for different combinations of CACC vehicles and

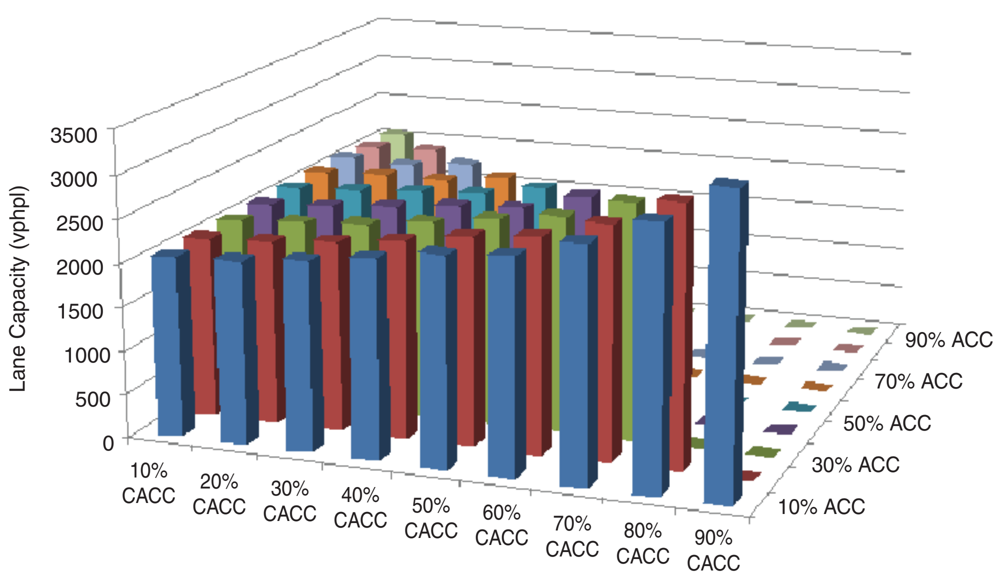

FIGURE 3 Updated prediction of lane capacity effects of ACC and CACC vehicles driven at time gaps chosen by drivers in field test (remaining vehicles manually driven).

TABLE 1 Updated Prediction of Lane Capacity Effects of ACC and CACC Vehicles Driven at Time Gaps Chosen by Drivers in Field Test

Percentage of ACC Vehicles	Lane Capacity (vph) by Percentage of CACC Vehicles								
	10%	20%	30%	40%	50%	60%	70%	80%	90%
10	2,065	2,090	2,170	2,265	2,389	2,458	2,662	2,963	3,389
20	2,065	2,110	2,179	2,265	2,378	2,456	2,671	2,977	0
30	2,077	2,127	2,179	2,269	2,384	2,487	2,710	0	0
40	2,088	2,128	2,192	2,273	2,314	2,522	0	0	0
50	2,095	2,133	2,188	2,230	2,365	0	0	0	0
60	2,101	2,138	2,136	2,231	0	0	0	0	0
70	2,110	2,084	2,155	0	0	0	0	0	0
80	2,087	2,101	0	0	0	0	0	0	0
90	2,068	0	0	0	0	0	0	0	0

NOTE: Remaining vehicles manually driven.

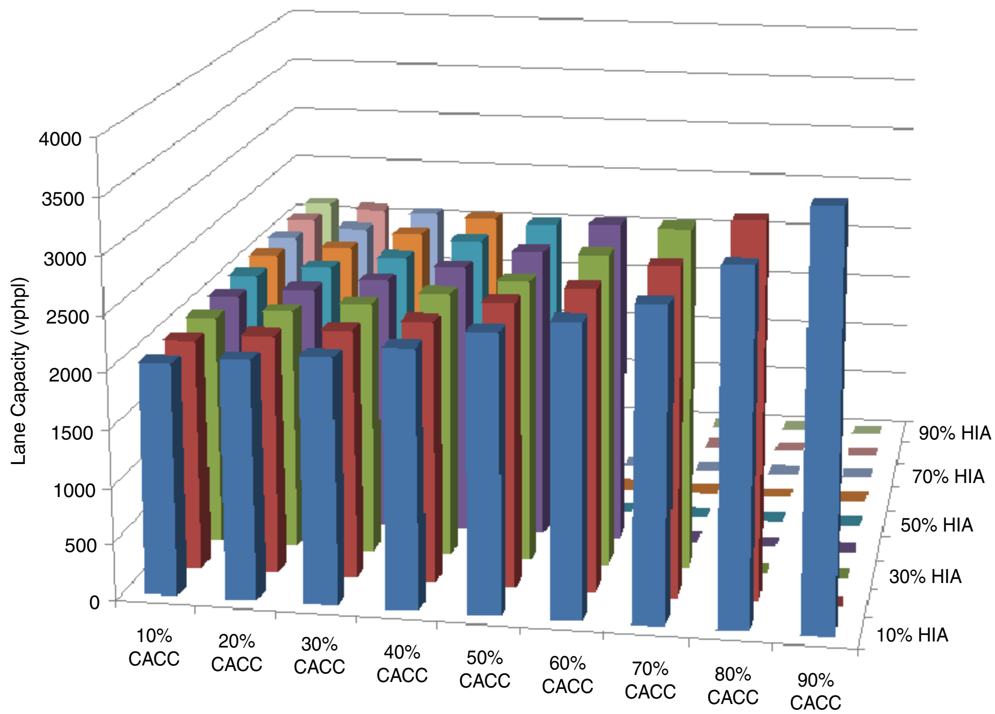

FIGURE 4 Prediction of lane capacity effects of VAD (HIA) and CACC vehicles driven at time gaps chosen by drivers in field test (remaining vehicles manually driven).

TABLE 2 Prediction of Lane Capacity Effects of VAD and CACC Vehicles Driven at Time Gaps Chosen by Drivers in Field Test

Percentage of VAD Vehicles	Lane Capacity (vph) by Percentage of CACC Vehicles								
	10%	20%	30%	40%	50%	60%	70%	80%	90%
10	2,045	2,110	2,179	2,288	2,447	2,576	2,760	3,111	3,624
20	2,054	2,125	2,211	2,323	2,512	2,671	2,893	3,303	0
30	2,064	2,148	2,246	2,378	2,519	2,787	3,041	0	0
40	2,073	2,165	2,282	2,434	2,611	2,891	0	0	0
50	2,084	2,187	2,318	2,503	2,685	0	0	0	0
60	2,097	2,206	2,362	2,545	0	0	0	0	0
70	2,102	2,227	2,395	0	0	0	0	0	0
80	2,114	2,252	0	0	0	0	0	0	0
90	2,123	0	0	0	0	0	0	0	0

NOTE: Remaining vehicles manually driven.

TABLE 3 Prediction of Lane Capacity Effects of VAD and CACC Vehicles Driven at Time Gaps Chosen by Drivers in Field Test

Percentage of VAD Vehicles	Lane Capacity (vph) by Percentage of CACC Vehicles								
	10%	20%	30%	40%	50%	60%	70%	80%	90%
10	2,086	2,132	2,168	2,278	2,443	2,567	2,831	3,108	3,624
20	2,135	2,164	2,207	2,366	2,446	2,669	2,941	3,303	0
30	2,137	2,193	2,291	2,364	2,533	2,775	3,041	0	0
40	2,128	2,206	2,302	2,439	2,588	2,891	0	0	0
50	2,139	2,220	2,324	2,499	2,685	0	0	0	0
60	2,134	2,239	2,373	2,545	0	0	0	0	0
70	2,137	2,245	2,395	0	0	0	0	0	0
80	2,132	2,252	0	0	0	0	0	0	0
90	2,123	0	0	0	0	0	0	0	0

NOTE: Remaining vehicles being ACC.

VAD vehicles (with the rest being conventional ACC vehicles) are shown in Table 3. Since the effects on capacity of ACC and manually driven vehicles are very similar, these results do not differ much from the previous results.

CONCLUDING REMARKS

The results reported here represent the first predictions of the effects of ACC and CACC on highway lane capacity that are founded on real experimental data from drivers who have driven the suitably equipped vehicles and selected the time gap settings with which they were comfortable. These results show that conventional ACC is unlikely to produce any significant change in the capacity of highways because drivers are only comfortable with the ACC system at gap settings similar to the gaps they choose when driving manually. In contrast, CACC has the potential to substantially increase highway capacity when it reaches a moderate to high market penetration because its higher dynamic response capabilities give drivers confidence that they can follow safely at significantly shorter gap settings, so they actually select those shorter gaps.

These results showed a maximum lane capacity of about 4,000 vph if all vehicles were equipped with CACC. If the vehicle population consists of CACC and VAD vehicles, meaning that all vehicles have been equipped with dedicated short-range communications radios, the lane capacity increases approximately linearly from 2,000 to 4,000 as the proportion of CACC vehicles increases from zero to 100%. However, if the vehicle population consists of manually driven and CACC vehicles, without any mandate for non-CACC vehicles to be equipped with dedicated short-range communications, the increase in lane capacity follows a quadratic profile, lagging significantly behind at the intermediate market penetration values. Therefore, the capacity benefits of CACC can be accelerated, or obtained at somewhat lower market penetrations, if the rest of the vehicle population is equipped with VADs so that they can serve as the lead vehicles for the CACC vehicles.

Further work will be needed to extend the models of ACC performance to include the full complexity of the dynamic response of real ACC systems, to represent their responses to strong traffic disturbances, and to show the ability of the combined ACC and driver system to respond safely to emergency stopping conditions even when driven at the short gaps enabled by CACC (which has already been demonstrated on test tracks).

ACKNOWLEDGMENTS

This research was conducted under the sponsorship of the State of California Business, Transportation, and Housing Agency; the California Department of Transportation; and FHWA's Exploratory Advanced Research Program, with additional support from Nissan Technical Center North America.

REFERENCES

1. Shladover, S. E., X.-Y. Lu, D. Cody, C. Nowakowski, Z. Qiu, A. Chow, J. O'Connell, J. Nienhuis, and D. Su. *Development and Evaluation of Selected Mobility Applications for VII.* Research Report UCB-ITS-PRR-2010-25. Partners for Advanced Transit and Highways (PATH), University of California, Berkeley, 2010. http://database.path.berkeley.edu/reports/index.cgi?reqtype=displayrecord&record=1011.
2. Nowakowski, C., S. E. Shladover, D. Cody, F. Bu, J. O'Connell, J. Spring, S. Dickey, and D. Nelson. *Cooperative Adaptive Cruise Control: Testing Drivers' Choices of Following Distances.* Research Report UCB-ITS-PRR-2011-01. PATH, University of California, 2011. http://database.path.berkeley.edu/reports/index.cgi?reqtype=displayrecord&record=1032.
3. Shladover, S. E., C. Nowakowski, J. O'Connell, and D. Cody. Cooperative Adaptive Cruise Control: Driver Selection of Car-Following Gaps. Presented at ITS World Congress, Busan, Korea, 2010.
4. Nowakowski, C., D. Cody, J. O'Connell, and S. E. Shladover. Cooperative Adaptive Cruise Control: Driver Acceptance of Following Gap Settings Less Than One Second. Presented at the Human Factors and Ergonomics Society 54th Annual Meeting, San Francisco, Calif., 2010.
5. VanderWerf, J., S. E. Shladover, M. A. Miller, and N. Kourjanskaia. Effects of Adaptive Cruise Control Systems on Highway Traffic Flow Capacity. In *Transportation Research Record: Journal of the Transportation Research Board, No. 1800,* Transportation Research Board of the National Academies, Washington, D.C., 2002, pp. 78–84.
6. Shladover, S., J. VanderWerf, M. A. Miller, N. Kourjanskaia, and H. Krishnan. *Development and Performance Evaluation of AVCSS Deployment Sequences to Advance from Today's Driving Environment to Full Automation.* Research Report UCB-ITS-PRR-2001-18. PATH, University of California, 2001. http://database.path.berkeley.edu/reports/index.cgi?reqtype=displayrecord&record=619.

7. van Arem, B., C. J. G. van Driel, and R. Visser. The Impact of Cooperative Adaptive Cruise Control on Traffic-Flow Characteristics. *IEEE Transactions on Intelligent Transportation Systems,* Vol. 7, No. 4, 2006, pp. 429–436.
8. Kesting, A., M. Treiber, M. Schönhof, and D. Helbing. Adaptive Cruise Control Design for Active Congestion Avoidance. *Transportation Research Part C,* Vol. 16, No. 6, Dec. 2008, pp. 668–683.
9. Kesting, A., M. Treiber, M. Schönhof, and D. Helbing. Extending Adaptive Cruise Control to Adaptive Driving Strategies. In *Transportation Research Record: Journal of the Transportation Research Board, No. 2000,* Transportation Research Board of the National Academies, Washington, D.C., 2007, pp. 16–24.
10. Schakel, W. J., B. van Arem, and B. D. Netten. Effects of Cooperative Adaptive Cruise Control on Traffic Flow Stability. *Proc., 13th International Annual Conference on Intelligent Transportation Systems,* Madeira Island, Portugal, IEEE, 2010, pp. 759–764.
11. Kesting, A., M. Treiber, and D. Helbing. Enhanced Intelligent Driver Model to Access the Impact of Driving Strategies on Traffic Capacity. *Philosophical Transactions of the Royal Society Series A,* Vol. 368, 2010, pp. 4585–4605.
12. *Aimsun Users Manual.* Transport Simulation Systems, New York, July 2009.
13. *Microsimulator and Mesosimulator in Aimsun 6 User's Manual.* Transport Simulation Systems, New York, April 2009.
14. *Aimsun Microsimulator API Manual.* Transport Simulation Systems, New York, July 2009.
15. *Aimsun Microscopic Simulator Behavioural Models SDK.* Transport Simulation Systems, New York, May 2008.
16. Bu, F., H.-S. Tan, and J. Huang. Design and Field Testing of a Cooperative Adaptive Cruise Control System. Presented at American Control Conference, Baltimore, Md., 2010.
17. Yeo, H. *Asymmetric Microscopic Driving Behavior Theory.* PhD dissertation. University of California, Berkeley, 2008.
18. Yeo, H., A. Skabardonis, J. A. Halkias, J. Colyar, and V. Alexiadis. Oversaturated Freeway Flow Algorithm for Use in Next Generation Simulation. In *Transportation Research Record: Journal of the Transportation Research Board, No. 2088,* Transportation Research Board of the National Academies, Washington, D.C., 2008, pp. 68–79.
19. Yeo, H., and A. Skabardonis. Parameter Estimation for NGSIM Freeway Flow Algorithm. *Proc., 10th Conference on Application of Advanced Technologies,* Athens, Greece, ASCE, New York, May 2008.

The contents of this paper reflect the views of the authors, who are responsible for the facts and accuracy of the data presented. The contents do not necessarily reflect the official views or policies of the State of California.

The Intelligent Transportation Systems Committee peer-reviewed this paper.